# A preliminary study on hydraulic resistance of bentonite/host-rock seal interface

Yong-Gui Chen, Yu-Jun Cui, Anh Minh A.M. Tang, Qiong Wang, Wei-Min Ye

# A preliminary study on hydraulic resistance of bentonite/host-rock seal interface

CHEN Yong-Gui[1, 2], CUI Yu-Jun[1, 2], TANG Anh Minh[2], WANG Qiong[2], YE Wei-Min[1]

1. Key Laboratory of Geotechnical and Underground Engineering of Ministry of Education and Department of Geotechnical Engineering, Tongji University, 1239 Siping Road, Shanghai 200092, PR China.

2. Laboratoire Navier/CERMES, Ecole des Ponts - ParisTech, 6-8 av. Blaise Pascal, Cité Descartes, 77455 Marne-la-Vallée, France.

**Corresponding author:**

Prof. CUI Yu-Jun

Laboratoire Navier/CERMES, Ecole des Ponts - ParisTech,

6-8 av. Blaise Pascal, Cité Descartes, 77455 Marne-la-Vallée, France.

Telephone : +33 1 64 15 35 50

Fax : +33 1 64 15 35 62

E-mail: yujun.cui@enpc.fr

ABSTRACT:

Compacted bentonite-based materials are often used as buffer materials in radioactive waste disposal. When the compacted bentonite blocks are emplaced, technological voids related to different interfaces involving the buffer material are created, and their hydro-mechanical behaviour is of primary importance for the disposal safety. In this study, the hydraulic resistance of the interface between compacted MX80 bentonite and Boom Clay was investigated in the laboratory using an injection cell. The results obtained show that when water is injected, the technological gap is quickly reduced due to the bentonite swelling. When water pressure reached the hydraulic resistance of the interface, the hydraulic fracturing took place with a drastic pressure decrease. After fracturing, water injection continued and bentonite continued to swell. A higher subsequent pressure was needed to produce a new hydraulic fracturing. After a certain time, the hydraulic resistance becoming high enough no further fracturing occured, suggesting that the technological gap was sealed.

Keywords : Clays, expansive soils, laboratory test, radioactive waste disposal

## INTRODUCTION

To safely dispose high-level radioactive waste (HLW), the deep geological repository concept has been adopted in several countries. For such repository at great depth, the buffer material employed to seal the waste canisters must have high swelling potential, low permeability and good adsorption capacity. Blocks made of compacted bentonite-based material are usually considered for this purpose.

When bentonite bricks are placed around the waste canisters in the sealing buffers, some technological voids either between the bricks themselves or between the bricks, the canisters and the host rock are created. For instance, 10 mm thick gaps between the bentonite blocks and canister and 25 mm thick gaps between the bentonite blocks and the host rock have been considered in the basic design of Finland (Juvankoski, 2010). The joint gaps are limited to 6.6% of the total volume of the confining structure in the FEBEX mock-up test (Martin et al., 2006). In France, the volume of the bentonite/rock gaps is estimated at 9% of the volume of the gallery by the French waste management agency (ANDRA, 2005), while this value reaches 14 % in the Tournemire Underground Research Laboratory (URL) site (Barnichon & Deleruyelle, 2009).

Once placed in the galleries, engineering barriers are progressively hydrated by pore water infiltration from the host rock. This water infiltration is strongly dependent on the initial state of the compacted material (Cui et al., 2008) and the imposed boundary conditions in terms of volume change (Yahia-Aissa et al., 2001). Thereby, the swell allowed by the technological voids described above has a significant influence on the hydro-mechanical behavior of the compacted bentonite. Indeed, swelling results in the decrease of dry density that may lead to the degradation of the hydro-mechanical performance of engineering barriers (Komine et al., 2009; Komine, 2010). Although the compacted bentonite swelling fills the technological gaps, the filled gaps still represent discontinuities over long time. As a result, the safety function expected in the design may not be properly ensured. Thereby, a good understanding of the interface gap behaviour under water pressure is essential.

In this study, three laboratory tests were conducted to evaluate the behaviour of the interface between compacted MX-80 bentonite and natural Boom Clay with different initial gaps. It is expected to provide useful information for the interface behaviour between bentonite blocks and host rock in the Praclay heating test conducted in the URL at Mol, Belgium.

## MATERIALS AND METHODS

The physical properties of MX80 bentonite and Boom Clay are shown in Table 1. A compacted MX80 bentonite block as those used in the Praclay heating test was employed with the dimensions shown in Figure 1. Its dry unit mass is 1.80 Mg/m$^3$, and its water content is 15.2%, defining a degree of saturation of 78.4%. The samples were prepared by coring from the block, and have a diameter of 50 mm or 55 mm and a height of 40 mm. Boom Clay cores taken from the Mol URL were used. The cores have a dry unit mass of 1.65-1.71 Mg/m$^3$, a water content of 21-25% and a degree of saturation of 91-100%. For the sample preparation, the core was first cut into small cylindrical pieces of 50 mm high and 100 mm diameter each using a metal saw. A mould was used to fix the cylindrical pieces, and a machine was employed to prepare a hole of 60 mm diameter. Afterwards, the two ends of the hollow cylinder sample was cut to have reach 40 mm height.

The experimental set-up is shown in Figure 2. The sample is placed inside a cell that is put in a rigid frame with a load transducer of 50 kN capacity that allows the measurement of axial stress. The water inlet at the bottom was connected to a controller of pressure/volume (CPV) for water injection. Inside the cell, a hollow cylinder of Boom Clay and a cylindrical bentonite specimen were installed. The space between the bentonite and Boom Clay samples allowed the technological gap to be simulated. The height of the samples was kept constant by blocking the piston.

A miniature total pressure sensor of 8 mm diameter and 2 mm thick was selected to monitor the radial pressure at the Boom Clay/bentonite interface (see Figure 3). Firstly, a small flat-bottomed hole with groove was prepared at the internal surface of Boom clay. Then the sensor was introduced into the hole and its cables were put into the groove. The scaning surface of the sensor was kept flush with the inner surface of Boom Clay. After the bentonite specimen was placed in the centre of the hollow cylinder of Boom Clay, the cables were connected to the data acquisition system. When water was introduced to the cell, the compacted bentonite was hydrated and radially swelled. The sensor recorded the generated pressure when the bentonite contacted Boom Clay.

Three tests with two different technological gaps were carried out on samples with the same initial water content and initial dry density (see Table 2). An initial axial stress of 0.5 MPa was applied on the specimen before hydration to ensure a good contact between the piston and the sample (see Figure. 2). When water injection started, the piston was fixed. In each test, the sample was hydrated by injecting distilled water under constant pressure (0.1 MPa) through a porous disk in contact with the bottom face, while the top face was put in contact with another porous stone so as to allow free expulsion of either air or water (see Figure 2). The outlet was closed when water flowed out of it. Once water was observed on the top of the cell, the rate of water injection was fixed at 1 $mm^3/s$. Changes in axial stress, radial pressures and injected water volume were monitored. When water pressure reached a certain value under which hydraulic fracturing occurred at the bentonite/Boom Clay interface, the water pressure decreased drastically. After the fracturing, the water injection was reset to the initial rate of 1 $mm^3/s$ until the next fracturing. This operation was repeated until no further hydraulic fracturing occurred. The dry density and water content of the soil specimen were determined at the end of the test.

## RESULTS AND DISCUSSION

Figure 4-6 show the changes in pressure, volume of water injected, axial and/or radial pressure. For all cases, when the injection pressure exceeded a certain level, a sudden decrease took place. This sharp decrease corresponds to the phenomenon of hydraulic fracturing, and this pressure level is called herein breakthrough pressure or hydraulic fracturing pressure.

Further examination shows that after starting water injection, the injection pressure started increasing after 1-2 h. In Test A, the first fracturing was observed at t = 15 h with a sharp pressure decrease from 2.9 MPa to 2.2 MPa. Afterwards, various hydraulic fracturing occured with an increase of the hydraulic resistance each time. When water was injected into the cell, it appeared to flow freely through the gap at the beginning. The water pressure did not increase before the gap was sealed by hydration that led the compacted bentonite to swell. Once the compacted bentonite was put in contact with water, it swelled and consequently reduced the gap. This sealing slowed down the water flow, resulting in an increase of the water pressure needed to keep a constant injection rate controlled by the CPV. When the water pressure reached the hydraulic resistance of the interface, hydraulic fracturing took place, resulting in a drastic pressure decrease. After fracturing, water was continued to be injected into the cell and bentonite continued to swell, thus, the hydraulic resistance was increased, resulting in a higher hydraulic fracturing pressure. Comparing the injection pressure in Test A to those on the two other tests, it appears clearly that the pressure in Test A increased more quickly than in Tests B and C due to the smaller gaps.

As for the axial pressure, it increased quickly just after starting the injection in relation to the bentonite swelling. When the fracturing was observed, the axial pressure also abruptly decreased. The hydraulic fracturings identified through the changes in injection pressure are thereby observed again. The trend of the axial pressure – time curves shows that the axial pressure in Test A with 2.5 mm gap increased more quickly than that in Tests B and C with 5 mm gap. In particular, once the injection was stopped in Test A, the axial pressure also dropped and a steady final pressure induced by hydration was observed. However, in Tests B and C, some mud was observed escaping from the top of the cell during the injection. At that moment, the axial pressure fluctuated following a similar trend as injection pressure , then they both decreased to zero. It is supposed that the larger gap resulted in a larger radial strain (10 mm/50 mm: 20%), and this deformation led to collapse of the compacted bentonite. As a result, the axial pressure abruptly decreased to zero, the injection water outflowed with the collapsed soil, and the injection pressure did not increase any more over time.

On the whole, the changes in radial pressure are in accordance with those in injection pressure. When water was injected into the cell, the bentonite swelled and the gap was reduced. Once the bentonite was in contact with Boom Clay, the radial pressure increased progressively. The sealing of the gap slowed down the water flow, resulting in the increase of water pressure. When the water pressure reached the hydraulic resistance of interface, a fracturing occurred and resulted in a drastic pressure decrease. If the hydraulic fracturing took place, a sudden decrease of the radial pressure was also produced.

On the other hand, various hydraulic fracturings on the radial pressure were also observed with the increase of fracturing pressure. This is in agrement with the observation of Marcial et al. (2006). The increase of radial pressure applied by the swelling bentonite on the internal surface of Boom Clay evidenced a rapid swelling rate. Logically, a gap of 2.5 mm in Test A was sealed more quickly than a gap of 5 mm in Tests B and C. In Test A, it was observed that the radial pressure reached 1.8 MPa when the water pressure was controlled at 0.2 MPa. This indicates that the hydration process was continued even though the water pressure was kept constant. Komine and Ogata (1999) reported that a necessary condition to demonstrate the self-sealing capability of buffer material is that the swelling pressure must be greater than 1 MPa once all voids are filled. Consequently, the interface between the Boom Clay and bentonite has enough swell capacity to seal a technical gap of 2.5 mm.

The distribution of water content and dry density of the soil samples after the tests are shown in Table 3. It appears that for each test the water content at the bottom was higher than that at the top. Moreover, the part near the interface was wetter than the other part. As for Boom Clay, the water content at the bottom was higher than that at the top, but the part near the cell was wetter than that near the gap. On the other hand, the dry density at the bottom and near the interface was lower than that at the top or far from the interface. This distribution is in good agreement with the wetting path. The difference between the results of Test A and Test B and C can be explained by the difference in gap thickness. In Test A, the diameter of the compacted bentonite was 55 mm and the gap was 2.5 mm, less bentonite was needed to fill the gap, and thereby a higher final dry density was obtained. Refering to Tests B and C, the difference in distribution might be due to the different volume of water injected and the different test durations. The fact that the water content and dry density were not uniform in the bentonite shows that the swelling of bentonite was not homogeneous.

## CONCLUSION

A simple experimental set-up was developed allowing investigation of the behaviour of the interface between Boom Clay and compacted MX-80 bentonite in terms of resistance to hydraulic fracturing. The obtained results allow the following conclusions to be drawn.

i) The water pressure did not increase at the first several hours after the start of injection until the gap was sealed by the compacted bentonite swelling. The axial pressure increased quickly in relation to the bentonite swelling, and it abruptly decreased when fracturing occured.

ii) When the gap was sealed, the radial pressure increased progressively. A sudden decrease of the radial pressure took place when hydraulic fracturing occurred. The fracturing pressure was found increasing over time.

iii) With a 2.5 mm gap, it was observed that fracturing pressure can be as high as 1.8 MPa that can be considered as high enough in the case of Boom Clay/compacted bentonite interface.

ii) The distribution of the water content and dry density of the soil after test depends on wetting path, gap thickness, injected water volume and elapsed time.

## ACKNOWLEDGEMENTS

ONDRAF/NIRAS (The Belgian Agency for Radioactive Waste and Enriched Fissile Materials) is gratefully acknowledged for its financial support. The authors are also grateful to the National Natural Science Foundation of China (No 41272287, 41030748), Innovation Program of Shanghai Municipal Education Commission (12ZZ032), Pujiang Program of Shanghai (13PJD029), and Fundamental Research Funds for the Central Universities.

## REFERENCES

Alonso E. E., Romero E. 2005. Expansive bentonite-sand mixtures in cyclic controlled-suction drying and wetting, Engineering Geology 81: 213-226.

ANDRA 2005. Référentiel des matériaux d'un stockage de déchets à haute activité et à vie longue – Tome 4: Les matériaux à base d'argilites excavées et remaniées, Rapport Andra N° CRPASCM040015B.

Barnichon J. D., Deleruyelle F. 2009. Sealing experiments at the Tournemire URL, Towards convergence of technical nuclear safety practices in Europe, EUROSAFE.

Blanchart P., Faure P., De Craen M., Bruggeman C., Michels R. 2012. Experimental investigation on the role of kerogen and clay minerals in the formation of bitumen during the oxidation of Boom Clay, Fuel 97: 344–351.

Bradbury M. H., Baeyens B. 2003. Porewater chemistry in compacted re-saturated MX-80 bentonite, Journal of Contaminant Hydrology 61: 329–338.

Chandler N., Dixon D., Gray M., Hara K., Cournut A., Tillerson J. 1998. The tunnel sealing experiment: an in situ demonstration of technologies for vault sealing, in Proceedings of the 19th Annual Conference of the Canadian Nuclear Society.

Cui Y. J., Tang A. M., Loiseau C., Delage P. 2008. Determining the unsaturated hydraulic conductivity of a compacted sand–bentonite mixture under constant-volume and free-swell conditions, Physics and Chemistry of the Earth 33: S462–S471.

Cui Y. J., Tang A. M., Qian L. X., Ye W. M., Chen B. 2011. Thermal-mechanical behavior of compacted GMZ bentonite, Soils and Foundations, 51(6): 1065-1074.

Delage P., Howat M., Cui Y. J. 1998. The relationship between suction and swelling properties in a heavily compacted unsaturated clay, Engineering Geology 50: 31–48.

Di Maio C. 1996. Exposure of bentonite to salt solution: Osmotic and mechanical effects, Geotechnique 46(4): 695-707.

Dixon D. A. 2000. Porewater salinity and the development of swelling pressure in bentonite-based buffer and backfill materials, POSIVA Report 2000-04, Posiva Oy, Helsinki, Finland.

Francois B., Laloui L., Laurent C. 2009. Thermo-hydro-mechanical simulation of ATLAS in situ large scale test in Boom Clay. Computers and Geotechnics 36: 626-640.

Gens A., Sánchez M., Guimarães L Do N, Alonso E E, Lloret A, Olivella S, Villar M V, Huertas F (2009) A full-scale in situ heating test for high-level nuclear waste disposal: Observations, analysis and interpretation, Geotechnique 59: 377-399.

Teachavorasinskun S, Visethrattana K (2006) Local hydraulic resistance of compacted sand-bentonite mixture, Geotechnical 56: 511-516.

Herbert H-J, Moog H C (1999) Cation exchange, interlayer spacing, and water content of MX-80 bentonite in high molar saline solutions, Engineering Geology 54, 55-65.

Hurel C, Marmier N (2010) Sorption of europium on a MX-80 bentonite sample: experimental and modelling results, Journal of Radioanal Nuclear Chemistry 284: 225–230.

Imbert C, Villar M V (2006) Hydro-mechanical response of a bentonite pellets/powder mixture upon infiltration, Applied Clay Science 32: 197-209.

Juvankoski M (2009) Description of Basic Design for Buffer, Working Report 2009-131, POSIVA OY.

Komine H (2004) Simplified evalution on hydraulic conductivities of sand-bentonite mixture backfill, Applied Clay Science 26: 13-19.

Komine H (2009) Self-sealing capability of some bentonite buffers in artificial seawater, Proceedings of the 17th International Conference on Soil Mechanics and Geotechnical Engineering, Hamza M et al.(Eds): 2495-2498.

Komine H, Ogata N (1996) Prediction for swelling characteristics of compacted bentonite, Canadian Geotechnical Journal 33(1): 11-22.

Komine H, Ogata N (1999) A Trial Design of Buffer Materials from the Viewpoint of Self-sealing (Tokyo: Central Research Institute of Electric Power Industry).

Lee J O, Lim J G, Kang I M, Kwon S (2012) Swelling pressures of compacted Ca-bentonite, Engineering Geology 129: 20-26.

Li X L, Bastiaens W, Marcke P Van, Verstricht J, Chen G J, Weetjens E, Sillen X (2010) Design and development of large-scale in-situ PRACLAY heater test and horizontal high-level radioactive waste disposal gallery seal test in Belgian HADES. Journal of Rock Mechanics and Geotechnical Engineering 2(2): 103–110.

Lloret A, Villar M V (2007) Advances on the knowledge of the therm-hydro-mechanical behaviour of heavily compacted “FEBEX” bentonite, Physysics and Chemistry of the Earth 32: 701-715.

Lloret A, Villar MV, Sanchez M, Gens A, Pintado X, Alonso EE (2003) Mechanical behaviour of heavily compacted bentonite under high suction changes, Geotechnique 53(1): 27-40.

Marcial D, Delage P, Cui Y J (2006) A laboratory study of the self-sealing behavior of a compacted sand-bentonite mixture. Geomechanics and Geoengineering: An International Journal 1: 73-85.

Martín P L, Barcala J M, Huertas F (2006) Large-scale and long-term coupled thermo-hydro-mechanic experiments with bentonite: the FEBEX mock-up test, Journal of Iberian Geology 32: 259-282.

Martino J B, Dixon D A, Kozak E T, Gascoyne M, Vignal B, Sugita Y, Fujita T, Masumoto K (2007) The tunnel sealing experiment: An international study of full-scale seals, Physics and Chemistry of the Earth 32: 93-107.

Mitachi T (2008) Mechanical behavior of bentonite-sand mixtures as buffer materials, Soils and Foundations 48(3): 363-374.

Montes-H G, Duplay J, Martinez L, Geraud Y, Rousset-Tournier B (2003) Influence of interlayer cations on the water sorption and swelling-shrinkage of MX-80 bentonite, Applied Clay Science 23: 309-321.

Nakashima Y (2006) H2O self-diffusion coefficient of water-rich MX-80 bentonite gels. Clay Minerals 41: 659-668.

Niu W J (2008) Study on unsaturated permeability of densely compacted bentonite under free swelling conditions. Ph.D-thesis, Tongji University, Shanghai.(in Chinese)

Tang A M, Cui Y J, Le T T (2008a) A study on the thermal conductivity of compacted bentonites, Applied Clay Science 41: 181–189.

Tang A M, Munoz J J, Cui Y J, Delage P, Li X L (2008b) Experimental evaluation of the hydraulic resistance of compacted bentonite/Boom clay interface, Proc. of the International Technical Conference on the Practical Aspects of Deep Geological Disposal of Radioactive Waste, Prague, 16-18 June 2008, pp. 16.1-16.9.(ISBN: 2-916162-05-4).

Villar M V (2006) Infiltration tests on a granite/Bentonite mixture: influence of water salinity, Applied Clay Science 31: 96-109.

Villar M V, Lloret A (2008) Influence of dry density and water content on the swelling of a compacted bentonite, Applied Clay Science 39: 38-49.

Wang Q, Tang A M, Cui YJ, Delage P, Gatmiri, B (2012) Experimental study on the swelling behaviour of bentonite/claystone mixture, Engineering Geology 124: 59-66.

Ye W M, Cui Y J, Qian L X, Chen B (2009) An experimental study of the water transfer through confined compacted GMZ bentonite, Engineering Geology 108: 169-176.

**List of Figures:**


Figure 1. Compacted bentonite block and cored sample

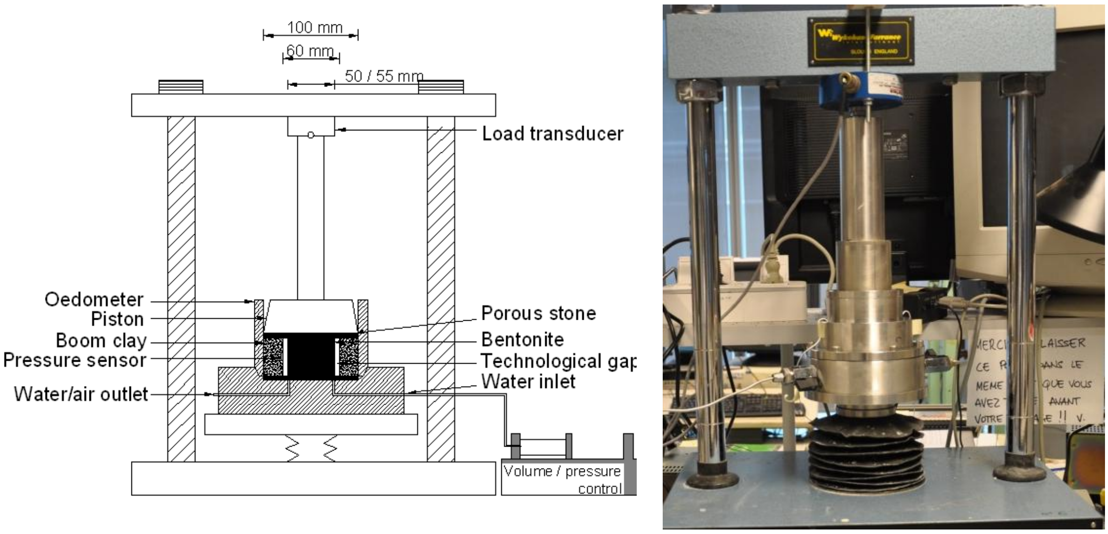


Figure 2. Schematic layout of the experimental set-up

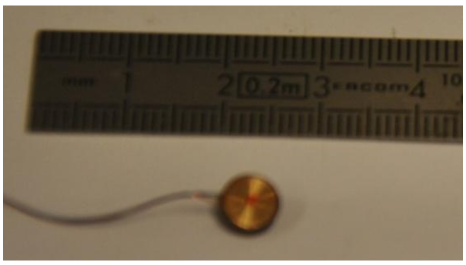

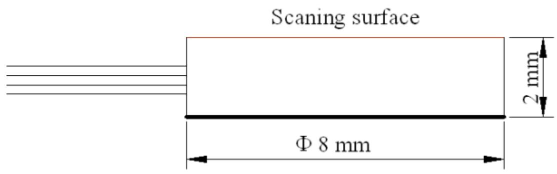


Figure 3. Miniature pressure sensor used

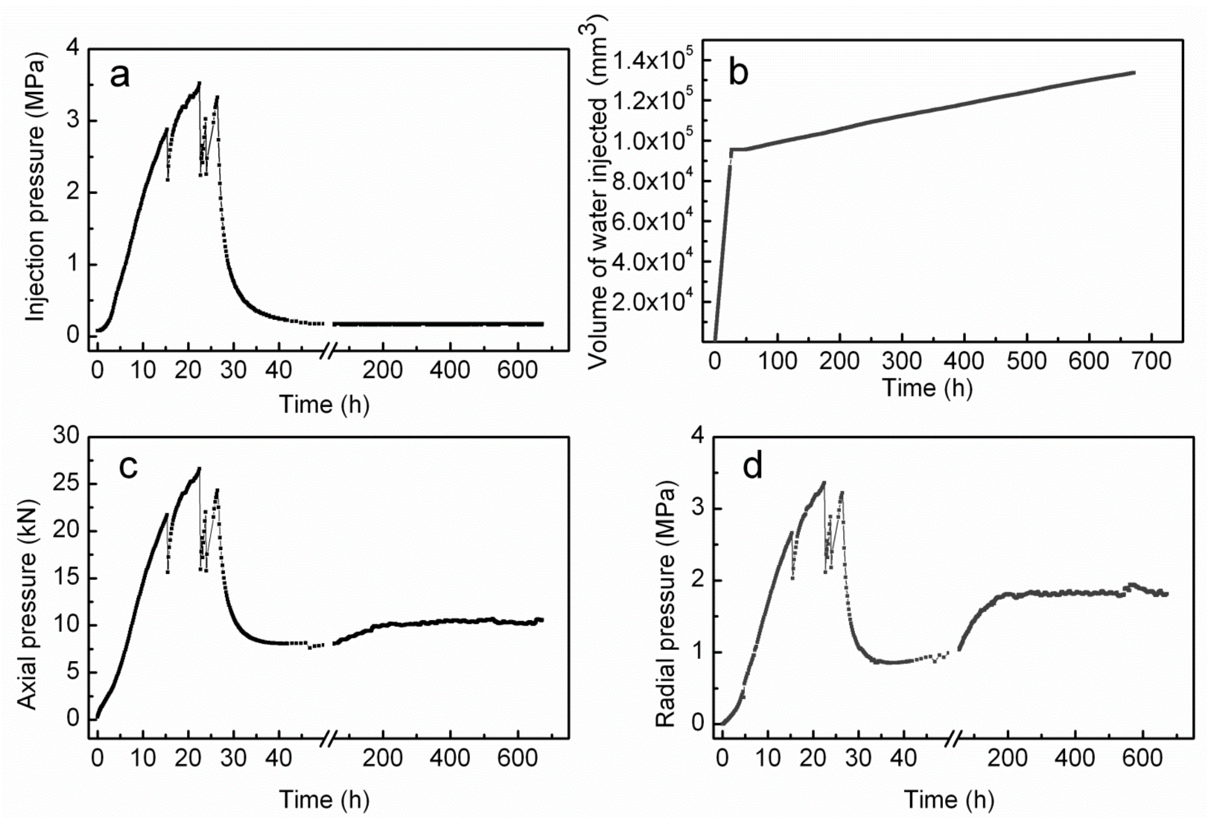


Figure 4. Changes in injection pressure (a), volume of water injected (b), axial (c) and radial (d) pressure in Test A

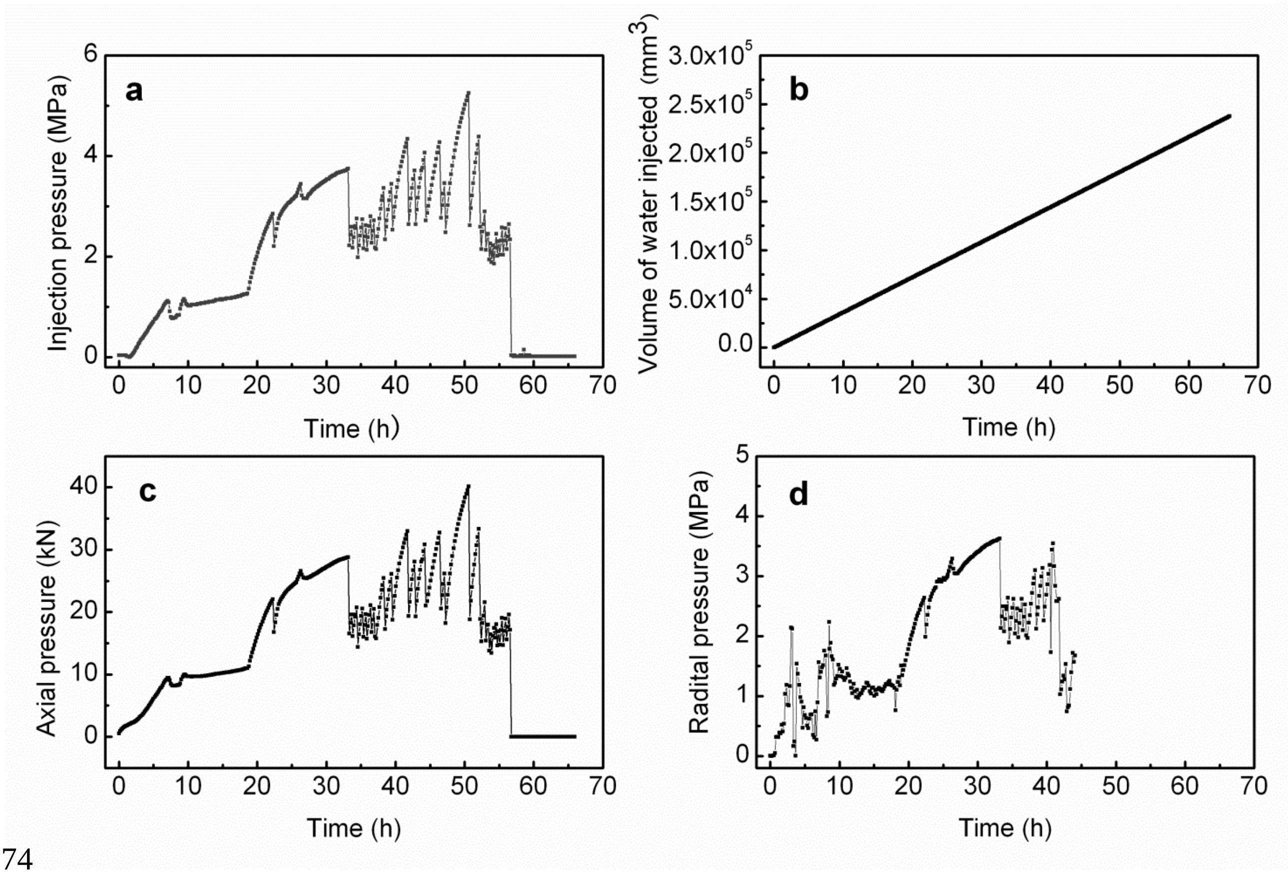


Figure 5. Changes in injection pressure (a), volume of water injected (b), axial (c) and radial (d) pressure in Test B

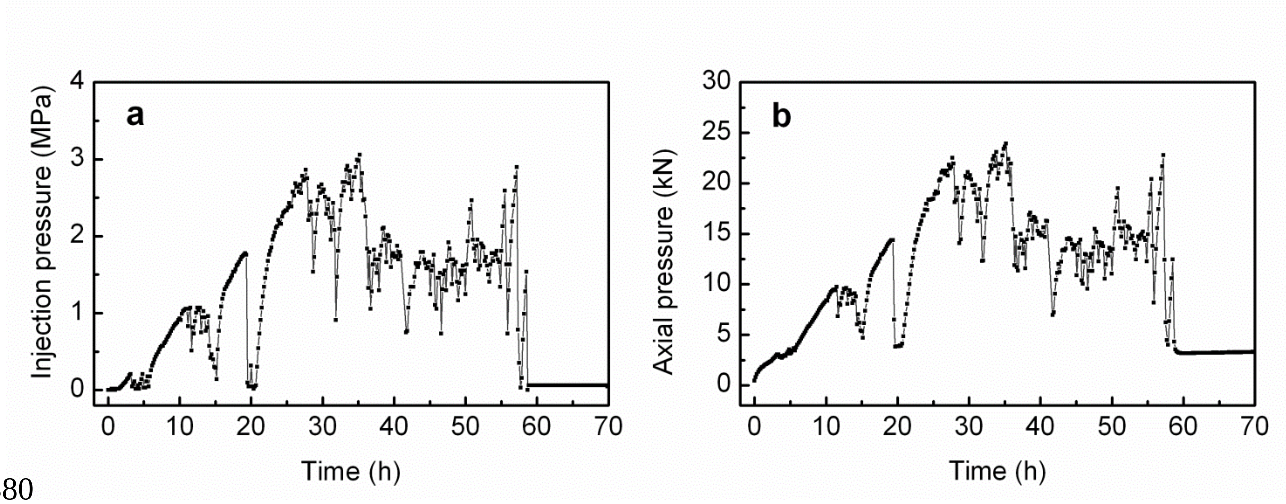


Figure 6. Changes in injection pressure (a) and axial pressure (b) in Test C

# Tables

Table 1. Mineralogical composition of the soils tested

| | MX80 bentonite (Wang et al. 2013) | Boom clay (Francois et al. 2009) |
|---|---|---|
| Montmorillonite (%) | 80 | 10 |
| Quartz (%) | | 60 |
| $w_l$ (%) | 575 | 59-83 |
| $w_p$(%) | 53 | 22-28 |
| $\rho_s$ (Mg/m$^3$) | 2.77 | 2.67 |

Table 2. Test conditions

| Test No. | Boom clay | | | | MX80 bentonite | | | Gap | |
|---|---|---|---|---|---|---|---|---|---|
| | Ex-diameter (mm) | Thickness (mm) | $\rho_d$ ($Mg/m^3$) | *w* (%) | Diameter (mm) | $\rho_d$ ($Mg/m^3$) | *w* (%) | Height (mm) | Thickness (mm) |
| A | 100 | 20 | 1.65 | 24 | 55 | 1.80 | 15.2 | 40 | 2.5 |
| B | 100 | 20 | 1.65 | 24 | 50 | 1.80 | 15.2 | 40 | 5 |
| C | 100 | 20 | 1.65 | 24 | 50 | 1.80 | 15.2 | 40 | 5 |

.

Table 3. Water content and dry density of the soil specimens after the tests

| | | w (%) | | | | $\rho_d$ (Mg/m$^3$) | | | | Test duration (hours) |
|---|---|---|---|---|---|---|---|---|---|---|
| | | $r_1$ | $r_2$ | $r_3$ | $r_4$ | $r_1$ | $r_2$ | $r_3$ | $r_4$ | |
| Test A | Top | 35 | 35.3 | 26.2 | 25.5 | 1.32 | 1.32 | 1.55 | 1.58 | |
| | Center | 35.1 | 39.0 | 26.4 | 26.3 | 1.54 | 1.30 | 1.54 | 1.57 | 680 |
| | Bottom | 40.1 | 42.2 | 28.6 | 28.2 | 1.09 | 1.24 | 1.48 | 1.48 | |
| Test B | Top | 37.1 | 44.3 | 37.0 | 29.8 | 1.25 | 1.21 | 1.39 | 1.48 | |
| | Center | 29.9 | 41.3 | 33.3 | 29.3 | 1.28 | 1.26 | 1.39 | 1.49 | 65 |
| | Bottom | 96.4 | 124.5 | 69.8 | 44.8 | 0.73 | 0.61 | 0.91 | 1.11 | |
| `Test C | Top | 43.2 | 45.5 | 28.5 | 29.1 | 1.34 | 1.22 | 1.50 | 1.47 | |
| | Center | 45.2 | 47.8 | 29.2 | 30.5 | 1.18 | 1.14 | 1.47 | 1.47 | 93 |
| | Bottom | 51.1 | 58.8 | 32.6 | 33.6 | 1.08 | 0.97 | 1.39 | 1.36 | |

*r*: the distance from the centre of the specimen to the sampling point; $r_1$=7.5mm, $r_2$=22.5mm, $r_3$=35mm, $r_4$=45mm.